



# Regulation of UCP1 expression by PPAR $\alpha$ and pemafibrate in human beige adipocytes

Pierre-Louis Batrow<sup>a</sup>, Christian H. Roux<sup>a,b</sup>, Nadine Gautier<sup>a</sup>, Luc Martin<sup>a</sup>, Brigitte Sibille<sup>a</sup>, Hervé Guillou<sup>c</sup>, Catherine Postic<sup>d</sup>, Dominique Langin<sup>e,f,g</sup>, Isabelle Mothe-Satney<sup>a</sup>, Ez-Zoubir Amri<sup>a,\*</sup>

<sup>a</sup> Université Côte d'Azur, CNRS, Inserm, Adipo-Cible Research Study Group, iBV, Nice, France

<sup>b</sup> Rheumatology Department, Hospital Pasteur 2 CHU, Adipo-Cible Research Study Group, Nice, France

<sup>c</sup> Toxalim (Research Centre in Food Toxicology), université de Toulouse, INRAE, ENVT, INP-Purpan, UPS, Toulouse, France

<sup>d</sup> Université Paris Cité, Institut Cochin, CNRS, Inserm, Paris, France

<sup>e</sup> Institute of Metabolic and Cardiovascular Diseases, I2MC, University of Toulouse, Inserm, Toulouse III University - Paul Sabatier (UPS), Toulouse, France

<sup>f</sup> Centre Hospitalier Universitaire de Toulouse, Toulouse, France

<sup>g</sup> Institut Universitaire de France (IUF), Paris, France

## ARTICLE INFO

### Keywords:

Beige adipocyte  
White adipocyte  
PPAR $\alpha$   
PPAR $\gamma$   
UCP1  
Pemafibrate

## ABSTRACT

**Aims:** Thermogenic adipocytes are able to dissipate energy as heat from lipids and carbohydrates through enhanced uncoupled respiration, due to UCP1 activity. PPAR family of transcription factors plays an important role in adipocyte biology. The purpose of this work was to characterize the role of PPAR $\alpha$  and pemafibrate in the control of thermogenic adipocyte formation and function.

**Materials and methods:** We used human multipotent adipose-derived stem cells and primary cultures of stromal-vascular fraction cells, transfected with siRNA against PPAR $\alpha$ , differentiated into white or beige adipocytes, by the treatment of rosiglitazone or pemafibrate. The expression of key marker genes of adipogenesis and thermogenesis was determined using RT-qPCR and Western blotting. An RNAseq analysis was also performed.

**Key findings:** We show that inhibition of PPAR $\alpha$  mRNA increases UCP1 mRNA and protein expression in beige adipocytes induced by rosiglitazone. Knock-down of PPAR $\alpha$  also increases stimulated glycerol release. Pemafibrate, described as a selective PPAR $\alpha$  modulator, induces adipogenesis and the expression of UCP1 in the absence of PPAR $\alpha$  expression. These effects are inhibited by a specific PPAR $\gamma$  antagonist highly suggesting that the pemafibrate effects in adipogenesis and beiging were mediated by PPAR $\gamma$ .

**Significance:** Conversion of white into thermogenic adipocytes is mainly due to the activation of PPAR $\gamma$ . Moreover, we show that PPAR $\alpha$  seems to act as a hindrance for PPAR $\gamma$ -dependent beiging. Our data question the role of PPAR $\alpha$  in human adipocyte browning and the specificity of pemafibrate in adipocytes.

## 1. Introduction

The prevalence of overweight and obesity continues to grow [1]. Obesity results from energy imbalance and affects the adipose organ. White adipose tissue (WAT) is specialized in energy storage/release in the form of lipids depending on metabolic needs whereas brown adipose tissue (BAT) burns fat to produce heat [2–4]. This thermogenic function of BAT mainly relies on the activity of uncoupling protein 1 (UCP1), a mitochondrial protein that uncouples the electron transport chain

activity from ATP synthesis [4]. UCP1-independent thermogenesis has been reported, it has been shown that UCP1 and creatine kinase B participate in thermogenesis [5–7]. UCP1 is present in classical brown adipocytes possessing multilocular lipid droplets and high mitochondrial density. However, adipocytes expressing UCP1 can be found within WAT after  $\beta$ -adrenergic stimulation or cold exposure [8], and these thermogenic cells are named beige or brite (brown in white) adipocytes. In the late 2000s, advances in imaging invalidated the admitted idea that, in humans, BAT disappeared with aging by putting in evidence the

\* Corresponding author at: iBV, Institut de Biologie Valrose, Université Côte d'Azur, CNRS UMR 7277, Inserm U1091, Tour Pasteur, Faculté de Médecine, 28 avenue de Valombrose, 06107 Nice, France.

E-mail address: [ez-zoubir.amri@univ-cotedazur.fr](mailto:ez-zoubir.amri@univ-cotedazur.fr) (E.-Z. Amri).

<https://doi.org/10.1016/j.lfs.2025.123406>

Received 14 October 2024; Received in revised form 15 January 2025; Accepted 16 January 2025

Available online 17 January 2025

0024-3205/© 2025 Elsevier Inc. All rights are reserved, including those for text and data mining, AI training, and similar technologies.

presence of thermogenic adipose tissue in healthy adult humans [9–11]. These thermogenic adipocytes originate either from de novo differentiation of precursor cells or conversion of mature white adipocytes [12,13].

The peroxisome proliferator-activated receptor (PPAR) family is involved in fatty acid oxidation and adipogenesis [14–16]. PPARs regulate gene transcription through binding to lipophilic ligands/activators, function as a heterodimeric complex with the retinoid X receptor (RXR), regulate various cellular activities, and are involved in several pathologies such as obesity, diabetes, neurodegenerative and cardiovascular diseases, and cancer [38; 39]. Three isoforms of PPARs ( $\alpha$ ,  $\beta/\delta$ ,  $\gamma$ ) have been described, with different functions and tissue expressions: PPAR $\alpha$  is the most expressed isoform in the liver among the three isoforms, while high levels of PPAR $\gamma$  are found in adipose depots. PPAR $\alpha$  is also highly expressed in BAT. Interestingly, PPAR $\alpha$  expression is low in WAT, but it increases during browning of white adipocytes upon cold exposure or treatment with CL316,243, a  $\beta$ 3-adrenergic receptor agonist [40], suggesting a role in WAT beiging. However, PPAR $\alpha$  seems dispensable for adipogenesis and cold-induced UCP1 expression as deletion of PPAR $\alpha$  in mice does not lead to any alteration in the WAT [40]. The role of PPAR $\alpha$  in the regulation of thermogenic capacity remains unclear, especially in humans, with very few data available in human models or in clinics.

PPARs endogenous ligands are lipids, but they remain to be identified, even though several studies have attempted to obtain crystallographic structures of the PPAR ligand-binding domain in complexes with endogenous fatty acids [17]. Synthetic PPAR activators/ligands have been developed during the early 1990s as these transcription factors represent an important class of drug targets. Studies have put in evidence the important role of the activation of PPAR family in the browning process [8,18]. Hence, numerous PPAR-activating compounds have been developed, although only a few of them are used in clinic. PPAR $\gamma$ -specific agonists thiazolidinediones such as rosiglitazone or pioglitazone are widely used in vitro to induce adipocyte differentiation and have been tested as insulin-sensitizers to treat patients with diabetes. However, adverse secondary effects, including heart failure, have pulled them out of the preferred drugs list in the treatment of hyperglycemia [19,20]. While the involvement of PPAR $\gamma$  in the browning of white adipocytes is well established, the importance of PPAR $\alpha$  activation in this process remains under debate. Treatment with rosiglitazone or GW7647 (a PPAR $\alpha$ -specific agonist) of human multipotent adipose-derived stem (hMADS) cells promotes the conversion of white adipocytes toward a thermogenic phenotype [18]. The use of compounds developed as relatively specific agonists of PPAR isoforms or pan-agonists have led to controversial data that are still the subject of debate [21,22]. Pemafibrate (also known as K-877) has been identified as a selective PPAR $\alpha$  modulator (SPPARM $\alpha$ ) with a very high affinity (Kd of 7 nM) and is used in clinics for the treatment of dyslipidemia [23–26]. Long-term exposure of mice to PPAR $\alpha$  agonist pemafibrate suppressed diet-induced obesity through the induction of hepatic FGF21 associated with browning of subcutaneous white adipocytes [27,28]. However, there is very little data available that describes direct effect of pemafibrate especially in humans.

In the present study we aimed at characterizing the involvement of PPAR $\alpha$  and/or its activation in the formation and function of beige adipocytes. To this end, we combined siRNA knock down and pharmacological treatment with specific PPAR $\alpha$  or PPAR $\gamma$  agonists as well as a PPAR $\gamma$  antagonist using human cell models of adipogenesis and white-to-beige conversion.

## 2. Materials and methods

### 2.1. Reagents

Cell culture media, insulin, and trypsin were purchased from Invitrogen (Cergy-Pontoise, France). Fetal bovine serum was from Eurobio

(Les Ulis, France). hFGF2 was from Peprotech (Thermo Fisher Scientific), and other reagents were from Cayman Chemical (Ann Arbor, MI, USA) or Sigma-Aldrich Chimie (Saint-Quentin-Fallavier, France).

### 2.2. Cell culture and stromal vascular fraction preparation

#### 2.2.1. hMADS cell culture

The establishment and characterization of human multipotent adipose-derived stem (hMADS) cells have previously been described [29,30]. Briefly, these cells, isolated from white adipose tissue removed from surgical scraps of infants undergoing surgery, did not enter senescence while exhibiting a diploid karyotype, were non-transformed though they expressed significant telomerase activity, did not show any chromosomal abnormalities after 140 population doublings (PDs), and maintained their differentiation properties after 160–200 PDs [30]. hMADS cells were able to withstand freeze/thaw procedures, and their differentiation could be directed under different culture conditions into various lineages. The cell population that has been studied here was isolated from the pubic region fat pad of a 4-month-old male donor (hMADS3). Cells were seeded at a density of 5000 cells/cm<sup>2</sup> in Dulbecco's Modified Eagle's Medium (DMEM) supplemented with 10 % Fetal Bovine Serum (FBS), 15 mM Hepes, 2.5 ng/mL human Fibroblastic Growth Factor (hFGF2), 60 mg/mL penicillin, and 50 mg/mL streptomycin. hFGF2 was removed when cells reached confluence. Differentiation was induced in a serum-free medium at day two post-confluence (designated as day 0, D0) in DMEM/Ham's F12 (1:1) media supplemented with 10  $\mu$ g/mL transferrin, 10 nM insulin, 0.2 nM triiodothyronine, 1  $\mu$ M dexamethasone, and 500  $\mu$ M isobutyl-methylxanthine for four days. Cells were treated between D2 and D9 with 100 nM rosiglitazone (#71740; Cayman Chemical), a PPAR $\gamma$  agonist, to enable white adipocyte differentiation. At D14, conversion of white to beige adipocytes was induced by a second rosiglitazone treatment for four days as previously described [18,31–33]. All compounds tested herein were added at D14. For some experiments, cells were treated with 100 nM of PPAR $\alpha$  agonist pemafibrate (#AX8R50; Interchim, Montluçon, France), or 3  $\mu$ M carbaprostacyclin (cPGI2, #18210, Cayman Chemical) to induce white-to-beige adipocyte conversion. One hundred or 300 nM of GW9662 (#70785, Cayman Chemical), a PPAR $\gamma$  antagonist, was added during the conversion periods for some experiments. Media was changed every other day, and cells were used at the indicated days.

#### 2.2.2. Human adipose tissue stroma-vascular fraction (SVF) preparation and culture

Abdominal subcutaneous human adipose tissue was collected from healthy patients undergoing surgeries (non-pathologic abdominoplasty) for SVF isolation according to the procedure previously described [34,35]. SVF cells were plated and maintained in DMEM containing 10 % FBS until confluence. Differentiation of primary cultures in white and beige adipocytes was performed according to the protocol described above for hMADS cells [18,35].

### 2.3. Oil Red O staining and quantification

Lipid accumulation was visualized by Oil Red O staining of 4 % formaldehyde-fixed hMADS adipocytes at D11 or D18. Lipid accumulation was quantified by eluting Oil Red O in 200  $\mu$ L of absolute ethanol. Optical density of 100  $\mu$ L of eluate was measured at 490 nm.

### 2.4. Transfection of siRNAs

PPAR $\alpha$  mRNA inhibition was performed by transfecting a 4-siRNA mix provided as a single reagent against human PPAR $\alpha$  (siPPAR $\alpha$ : Dharmacon: L-003434-00-0005), or a non-targeting siRNA (siCtrl; ON-TARGETplus Non-targeting Control Pool) for qPCR and Western-blot analysis (Dharmacon: D-001810-10-05); three controls (siGFP, NOSiRNA and non-transfected cells) for RNAseq analysis) as a control.

Briefly, hMADS cells at D10 were incubated with a mixture containing Lipofectamine RNAiMAX Transfection Reagent and siRNA (25 nM) in Opti-MEM Reduced Serum Medium. After 24 h, the transfection medium was replaced by the differentiation medium.

## 2.5. RNA isolation and analysis

Cells were lysed in Tri-Reagent solution according to the manufacturer's instructions and stored at  $-80^{\circ}\text{C}$  till analysis. These procedures followed Minimum Information for Publication of Quantitative Real-Time PCR Experiments (MIQE) standard recommendations and were conducted as described previously [36]. The oligonucleotide sequences, designed using Primer Express software, are shown in Supplementary Table S1. Quantitative PCR (qPCR) was performed using ONEGreen® Fast qPCR Premix (Ozyme, Saint-Cyr-l'École, France), and assays were run on a StepOne Plus ABI real-time PCR machine (PerkinElmer Life and Analytical Sciences, Boston, MA, USA). The expression of selected genes was normalized to that of the 36B4 housekeeping gene and then quantified using the comparative- $\Delta\text{Ct}$  method.

## 2.6. RNA sequencing (RNA-seq) analysis

To assess the transcriptome differences between hMADS cells expressing or not *PPAR $\alpha$* , three biological replicates were sequenced, three controls (siGFP, NosiRNA and non-transfected cells) were used. Before further analysis, RNA integrity number was verified ( $\text{RIN} > 8$ ). All mRNA library preparation, quality examination, and RNA sequencing were conducted by GENEWIZ France Ltd. Functional annotation of gene ontology (GO) enrichment, Kyoto Encyclopedia of Genes and Genomes (KEGG), and clustering analysis were performed from read counts with iDEP 2.0 web application (Integrated Differential Expression & Pathway analysis) using edgeR and DESeq2 packages [37]. FASTQ data have been deposited on BioStudies and are accessible through accession number E-MTAB-12937.

## 2.7. Lipolysis assays

Lipolysis was assessed by measuring glycerol release from differentiated cells at D18. Differentiated adipocytes were insulin-deprived for 60 min; then, fresh medium was added and the cells were immediately subjected to  $1\ \mu\text{M}$  isoproterenol, a pan  $\beta$ -adrenergic receptor agonist, for 90 min. The sampled medium was used to measure glycerol release with a glycerol colorimetric assay kit (Cayman), according to the manufacturer's instructions. The results were normalized to the protein amount.

## 2.8. Western blot analysis

Proteins were extracted from cells or tissues as previously described [38]. Equal amounts of cellular proteins, 30 to 50  $\mu\text{g}$ , were separated by electrophoresis using gradient gels (4–15 %) and blotted onto PVDF membranes. Following blocking, membranes were incubated with primary antibody overnight at  $4^{\circ}\text{C}$  (anti-UCP1, Abcam #ab10983, dilution 1:1000; anti-TBP, CST #D5C9H, dilution 1:1000; anti pan-ACTIN, CST #8456, dilution 1:1000). Primary antibodies were detected with HRP-conjugated anti-rabbit or anti-mouse immunoglobulins (Promega, Madison, WI, USA). Chemiluminescence obtained after adding Immobilon Forte Western HRP substrate (Merck-Millipore, Burlington, MA, USA) was detected using an Amersham Imager 600 (GE HealthCare, Chicago, IL, USA) and quantified with ImageJ.

## 2.9. Statistical analyses

Statistical analyses were performed using Prism 9.1.1 software (GraphPad Software, Dotmatics, Boston, MA, USA). Data statistical differences between experimental groups were analyzed by one-way ANOVA followed by Šidák's post hoc test or two-way ANOVA followed

by Tukey when appropriate. Data are expressed as mean values  $\pm$  SEM as relative expression of control white adipocyte, unless otherwise described in legend. Differences were considered statistically significant when  $P < 0.05$ .

## 3. Results

### 3.1. Transcriptomic analysis confirmed the metabolic reprogramming induced by rosiglitazone and revealed that *PPAR $\alpha$* mRNA silencing enhances the expression of *UCP1* in hMADS beige adipocytes

While it is well established that activation of *PPAR $\gamma$*  is important to induce the conversion of white adipocytes into beige ones, the role of *PPAR $\alpha$*  in this process remains unclear. Here, we aimed to investigate the role of *PPAR $\alpha$*  in the rosiglitazone-dependent beiging process by inhibiting its expression before the induction of adipocytes conversion. *PPAR $\alpha$*  mRNA silencing was performed on the 10th day of differentiation (D10) and cells were induced to convert in the presence of 100 nM rosiglitazone at D14 for 4 days.

Transcriptomic analysis of white and beige hMADS adipocytes indicated a marked effect of rosiglitazone on overall gene expression, as revealed by principal component analysis (Fig. 1A) where all cells treated with rosiglitazone clustered together. Gene and KEGG pathways enrichment confirmed metabolic reprogramming, including in *PPAR* signaling and fatty acid metabolism upon rosiglitazone treatment (Fig. 1B). siGFP and siPPAR $\alpha$  groups clustered together, indicating a similar overall gene expression profile in the two groups. Extended RNAseq analysis revealed little changes after *PPAR $\alpha$*  silencing in white or beige adipocytes as only a few genes were differentially expressed in adipocytes downregulated for *PPAR $\alpha$*  compared to control ones (siPPAR $\alpha$  vs siGFP; Fig. 1C). Of note, data analysis revealed that *UCP1* expression increased upon inhibition of *PPAR $\alpha$*  expression in beige adipocytes (Fig. 1D). This increase upon *PPAR $\alpha$*  expression inhibition was unexpected in view of previous data obtained in hMADS adipocytes treated with *PPAR $\alpha$*  agonist, GW7647 [18]. This observation required further investigations and confirmations.

### 3.2. *PPAR $\alpha$* mRNA silencing enhances the expression of *UCP1* in converted beige adipocytes

To further decipher the effects of *PPAR $\alpha$*  downregulation in white and converted beige adipocytes, we performed qPCR analyses on siCtrl and siPPAR $\alpha$  transfected cells. First, we confirmed siRNA inhibition of *PPAR $\alpha$*  expression in both white and beige adipocytes with a 90 % decrease of *PPAR $\alpha$*  mRNA levels (Fig. 2A). On the contrary, the expression of the other *PPAR* isoforms ( $\delta$  and  $\gamma 2$ ) did not present any significant variation upon *PPAR $\alpha$*  downregulation (Fig. 2A). In these conditions, the expression of adipogenic markers (*Plin1* and *Fabp4*) was not affected by the silencing of *PPAR $\alpha$*  expression (Fig. 2B). *UCP1* mRNA expression in beige hMADS adipocytes induced by rosiglitazone was 60 % higher in the absence of *PPAR $\alpha$*  expression compared to siCtrl (Fig. 2C). This increase in *UCP1* mRNA expression was associated with a similar increase at the protein level (Fig. 2D). Except for *UCP1*, other thermogenic (*CPT1M*, *CIDEA*, *GK*) markers expression was not affected by the inhibition of *PPAR $\alpha$*  expression (Fig. 2E). Among few candidate genes that were affected by the inhibition of *PPAR $\alpha$*  expression, *KCNK3*, *MCU*, *TAP1* and *NLRC5* were identified as potentially differentially expressed by RNAseq analysis (Fig. 1D). However, qPCR analysis of *KCNK3*, *MCU* and *TAP1* did not revealed any differences upon inhibition of *PPAR $\alpha$*  expression (Supplementary Fig. 1A), while *NLRC5* only showed tendencies for increased expression (Fig. 2F).

To further characterize the effect of *PPAR $\alpha$*  mRNA silencing, we investigated thermogenic associated functions such as lipolysis. Isoproterenol-stimulated glycerol release was increased in beige adipocytes downregulated for *PPAR $\alpha$*  compared to basal glycerol release in beige cells treated with siCtrl (Supplementary Fig. 1B). Basal lipolysis

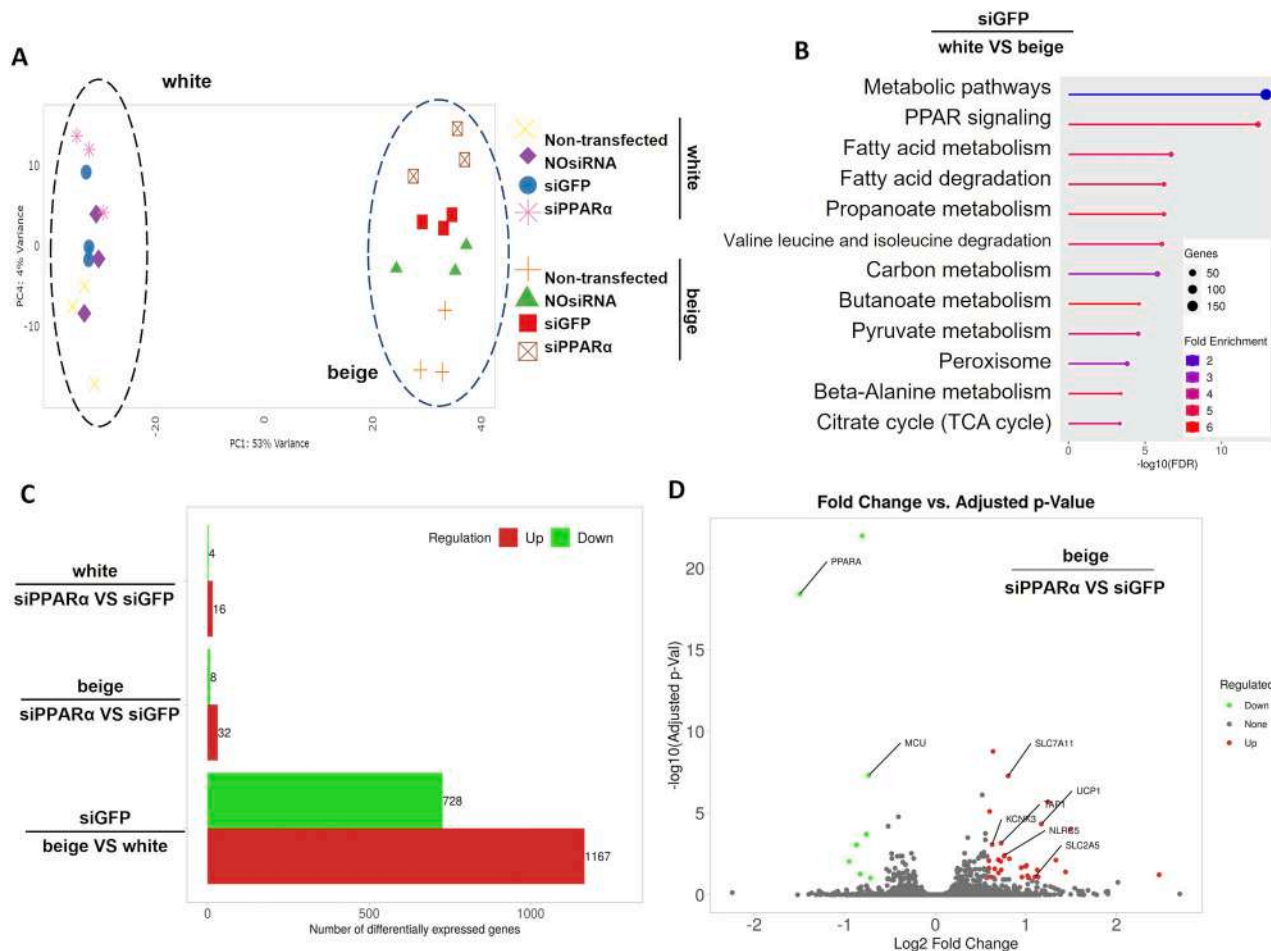


**Fig. 1.** Transcriptomic analysis confirmed the metabolic reprogramming induced by rosiglitazone and revealed that PPARα mRNA silencing enhances the expression of UCP1 in hMADS beige adipocytes.

Transcriptomic analysis of hMADS adipocytes transfected with different siRNAs at D10 after differentiation and then induced to convert to beige adipocyte on D14 in the presence of 100 nM rosiglitazone. (A) Principal component analysis. (B) Gene and KEGG metabolic pathways enrichment upon rosiglitazone treatment. (C) Numbers of differentially expressed genes, down (green) and up-regulated (red) upon siRNA transfection in white or beige hMADS adipocytes. (D) Volcano plot from RNAseq data (FDR cutoff: 0.1, min fold-change: 1.5).

was not modified. In white adipocytes, inhibition of *PPARα* slightly increased isoproterenol-stimulated glycerol release without reaching significant level (Supplementary Fig. 1B). Furthermore, as UCP1 is a mitochondrial protein, we investigated the relative mitochondrial DNA content in adipocytes treated with siPPARα. Of note, mitochondrial DNA content increased upon rosiglitazone treatment, and *PPARα* inhibition led to a further increase in agreement with the increase in *UCP1* mRNA and protein content (Supplementary Fig. 1C and Fig. 2C and D).

### 3.3. Effects of PPARα silencing is consistent in various models of beiging

To determine whether the Ucp1 induction in thermogenic adipocytes observed in hMADS cells was specific or not to these cells, we investigated the role of PPARα in another human adipocyte model. We performed silencing experiments in primary cultures of adipocytes derived from human stroma-vascular fraction (hSVF) in a similar way than in hMADS cells. Inhibition of *PPARα* expression reached the same efficiency in both cell types (90 % decreases). In addition, we found that, as observed in hMADS-derived adipocytes, inhibition of PPARα expression increased *UCP1* mRNA level by 60 % in beige adipocytes induced with 100 nM of rosiglitazone while classical white adipocyte marker *PLIN1* expression was not modified (Fig. 3A).

To ensure that this effect was not rosiglitazone-dependent, we used carbaprostacyclin (cPGI2), a stable analog of prostacyclin, to induce

white to beige adipocyte conversion in hMADS derived adipocytes as described previously [32]. siRNA *PPARα* silencing also allowed the induction of *UCP1* expression by 46 % upon cPGI2 treatment compared to siCtrl-transfected adipocytes (Fig. 3B). Similar results were obtained in primary cultures of adipocytes derived from human stroma-vascular fraction treated with cPGI2 (data not shown). These results indicate that *PPARα* silencing enhances beiging in two models of human adipocyte independently of browning inducers used.

### 3.4. PPARγ antagonist GW9662 alleviates UCP1 induction of beige adipocyte triggered by PPARα mRNA silencing

To unravel the crosstalk between PPARα and PPARγ at play upon white-to-beige adipocyte conversion, we blocked PPARγ action with the GW9662 specific antagonist in hMADS-derived adipocyte treated with siPPARα and converted through rosiglitazone treatment. Measure of *UCP1* mRNA showed a dose-dependent decrease in siCtrl-expressing beige cells, indicating that GW9662 treatment inhibited the conversion of adipocytes induced by rosiglitazone (Fig. 4A, grey bars). As shown above, *PPARα* mRNA silencing induced an increase of *UCP1* expression in beige hMADS adipocytes, both at the mRNA and protein levels (Fig. 2C and D and Fig. 4A). UCP1 mRNA and protein dosage showed that this induction was inhibited by GW9662 treatment in a dose-dependent-manner (Fig. 4A, pink bars on left panel, and right



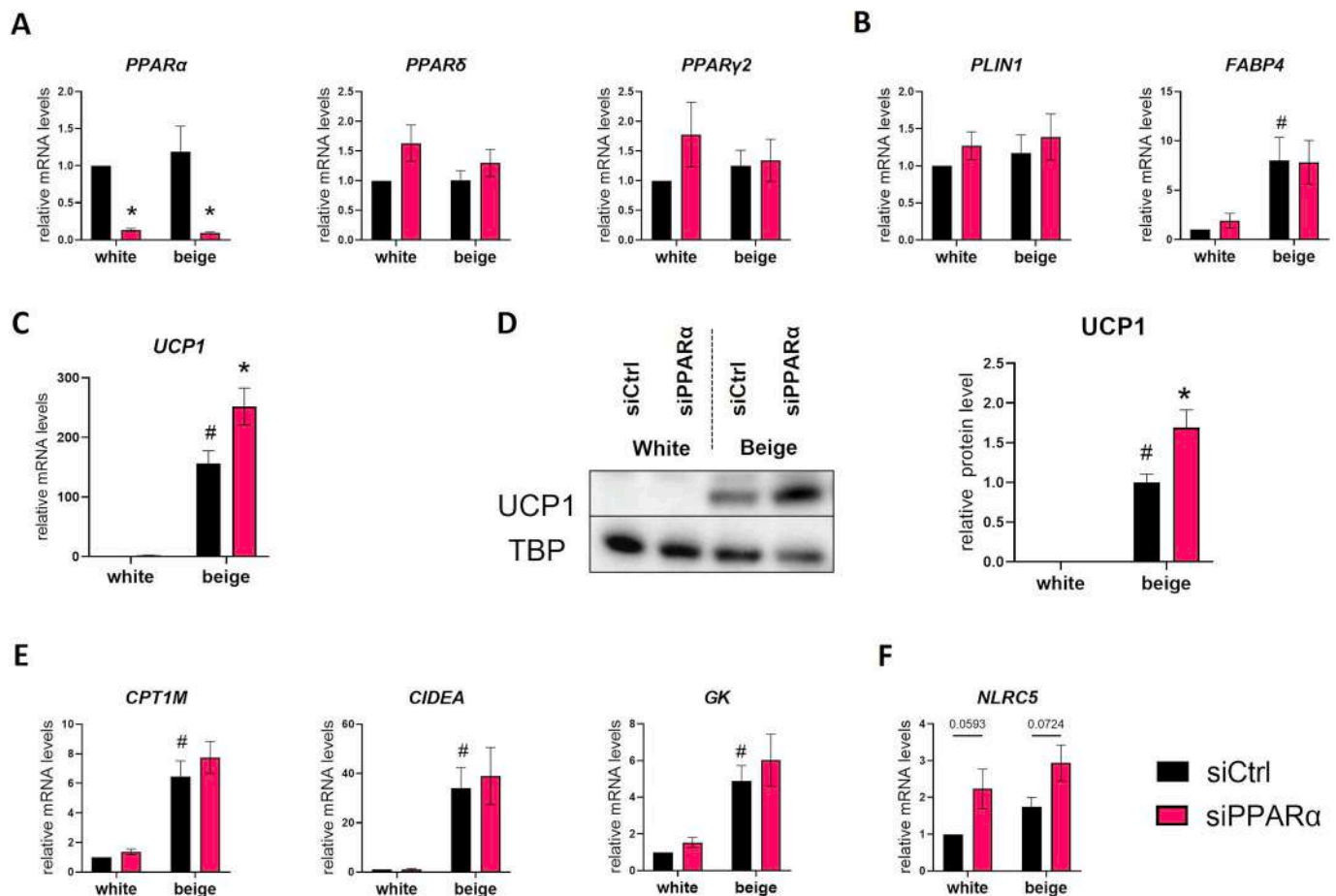


**Fig. 2.** *PPARα* mRNA silencing enhances the expression of UCP1 in hMADS beige adipocytes. hMADS cells were induced to differentiate into adipocyte, transfected with siRNA (black bars siCtrl and pink bars siPPARα) at D10. At D14, cells were induced or not to convert into beige adipocytes using 100 nM rosiglitazone. (A) *PPARs*, (B) adipogenic markers *PLIN1* and *FABP4*, (C) UCP1 mRNA levels were measured. (D) 40 µg total protein extracts were analyzed by Western blot. For UCP1 content, (E) Thermogenic markers *CPT1M*, *CIDEA*, *GK*, (F) *NLRC5* mRNA levels were measured. Histograms display mean ± SEM of 9 independent experiments except 3 for (D). Statistics by two-way ANOVA with Tukey's multiple comparisons test,  $p < 0.05$  considered as significant: #, vs white siCtrl; \*, vs beige siCtrl.

panel). Moreover, the expression of other *PPARγ* targets such as *CPT1M* or *FABP4* tended to be reduced by GW9662 in beige adipocytes transfected with both siPPARα and siCtrl (Fig. 4B). Adipogenic marker *PLIN1* expression was not affected by *PPARγ* antagonist (Fig. 4B). The levels of the other *PPAR* isoforms (δ and γ2) were not modified by the inhibition of *PPARα* expression nor the treatment with GW9662 (Fig. 4C). Altogether, these data suggest that *PPARα* could act as a negative modulator in *PPARγ*-dependent beiging of human adipocyte.

### 3.5. Pemaifibrate induces UCP1 expression in human white adipocytes

*PPARα* agonists have been developed with low specificity at least in the adipocyte context, and pemaifibrate has been identified as the most selective *PPARα* modulator (SPPARMα) on the market, with an EC50 around 7 nM [39,40]. We aimed to investigate the contribution of *PPARα* to beiging at a pharmacological level as inhibition of its expression led to an enhanced rosiglitazone-induced UCP1 expression. For this purpose, hMADS cells were differentiated into white adipocytes for 14 days and then treated with various amounts of pemaifibrate for 4 days. hMADS adipocytes treated with similar doses of rosiglitazone were used as controls. Rosiglitazone and pemaifibrate treatments did not affect the morphological shape of the cells, nor did they affect their lipid content as shown by Oil Red O staining (Fig. 5A). Treatment with 100 nM of pemaifibrate induced the expression of UCP1 at the protein level (Fig. 5B), but to a lesser extent than rosiglitazone (50 %). Pemaifibrate also increased the mRNA level of several thermogenic markers such as

*UCP1*, *CPT1M*, *PDK4* and *ANGPTL4* (Fig. 5C). However, pemaifibrate treatment was not as effective as rosiglitazone: higher doses were required to reach similar levels (Fig. 5C). Pemaifibrate is able to promote adipocyte beiging with a lower potency than rosiglitazone. The expression of the three *PPAR* isoforms (α, β, γ2) was not altered by pemaifibrate or rosiglitazone treatment (Fig. 5D). Finally, simultaneous treatment with both activators (rosiglitazone and pemaifibrate) did not lead to any additive or synergistic effects, suggesting that both compounds use the same signaling pathway (Supplementary Fig. 2).

### 3.6. *PPARγ* antagonist GW9662 interferes with *PPARα* activation induced by pemaifibrate

As both *PPARα* and *PPARγ* are expressed in adipocytes, we then aimed to characterize whether pemaifibrate effects were indeed mediated by *PPARα* activation. To this purpose, we treated hMADS white adipocytes with pemaifibrate in the presence of various amounts of *PPARγ* antagonist (GW9662). Cells treated with rosiglitazone were used as controls. As expected, UCP1 induction by rosiglitazone was inhibited by GW9662 treatment (Fig. 6A). Unexpectedly, the expression of UCP1 by pemaifibrate was also affected by the *PPARγ* antagonist at all doses (Fig. 6A). Rosiglitazone and pemaifibrate effects were also observed at the protein level as UCP1 protein content decreased in a dose dependent manner in the presence of GW9662 (Fig. 6A bottom). The level of other *PPARγ* target genes such as *FABP4* and *CPT1M* was also slightly decreased by 300 nM of GW9662. *PLIN1* expression, which is not a *PPAR*

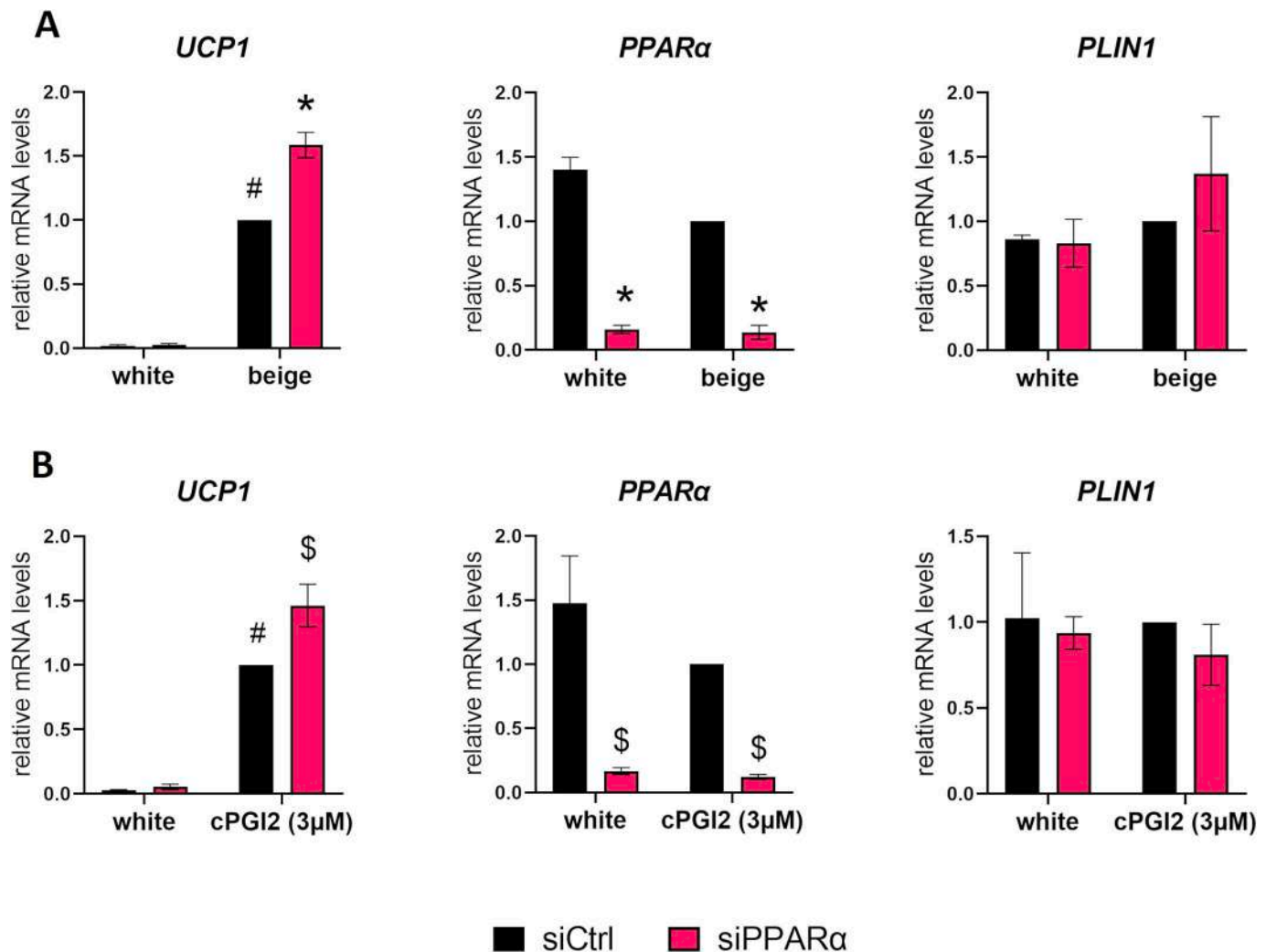


**Fig. 3.** Effects of PPAR $\alpha$  silencing is consistent in various models of beigeing

SVF cells derived from human subcutaneous tissue (A) or hMADS cells (B) were induced to differentiate, transfected at D10 and then induced to convert into beige adipocytes at day14 for the last 4 days in the presence of 100 nM rosiglitazone (A) or 3  $\mu$ M cPGI2 (B). mRNA levels of thermogenic and adipogenic markers were analyzed. Histograms display mean  $\pm$  SEM of 3 independent experiments. Statistics by two-way ANOVA with Tukey's multiple comparisons test,  $p < 0.05$  considered as significant: #, vs white siCtrl; \*, vs beige siCtrl, \$, vs cPGI2 siCtrl.

target, was not affected (Fig. 6B). The expression of the three PPARs was not affected (Fig. 6C).

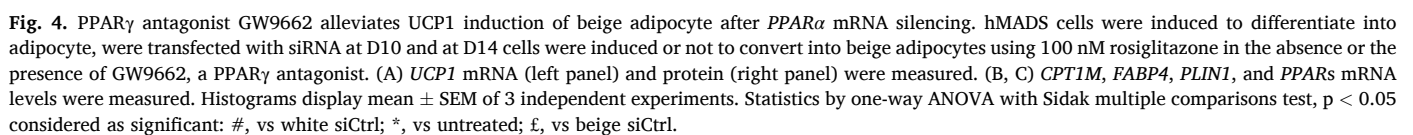
In order to validate these observations, we tested the effects of pemafibrate in hSVF cells differentiated into white adipocytes and treated with 100 nM of rosiglitazone or pemafibrate in the presence of various amounts of GW9662 (Fig. 6D). In agreement with results obtained in hMADS adipocytes, pemafibrate-induced UCP1 and CPT1M expression was inhibited by the PPAR $\gamma$  antagonist GW9662 similarly to that induced by rosiglitazone. Our observations question the specificity of pemafibrate for PPAR $\alpha$  in an adipose context. Altogether, our findings suggest an effect of pemafibrate mainly through the activation of PPAR $\gamma$ .

### 3.7. Effects of pemafibrate on adipocytes are likely due to PPAR $\gamma$ activation

Induction of thermogenic markers by pemafibrate in hMADS white adipocytes is abolished by PPAR $\gamma$  antagonist, suggesting that its beigeing effect may not be mediated through PPAR $\alpha$ . To test this hypothesis, we transfected hMADS white adipocytes with siRNA against PPAR $\alpha$  at D10, then treated the cells simultaneously with pemafibrate and GW9662 for four days. At D18, PPAR $\alpha$  mRNA level was decreased by 92 % in siPPAR $\alpha$  compared to cells treated with siCtrl (Fig. 7A, left). Of note,

PPAR $\delta$  and PPAR $\gamma$ 2 expression was not affected by the downregulation of PPAR $\alpha$  (Fig. 7A, right). This strong inhibition of PPAR $\alpha$  expression did not affect pemafibrate-dependent induction of UCP1 mRNA and protein (Fig. 7B). However, this induction was inhibited by the PPAR $\gamma$  antagonist GW9662 in the presence or absence of PPAR $\alpha$  (Fig. 7B). Consistently, the expression of PPAR $\gamma$ -target genes CPT1M and FABP4 was reduced by PPAR $\gamma$  antagonist in both adipocytes transfected with siCtrl or siPPAR $\alpha$ , whereas PLIN1 was not (Fig. 7C).

As our observations strongly suggest that pemafibrate induces adipocyte beigeing through PPAR $\gamma$  and not PPAR $\alpha$ , we asked whether pemafibrate was able to induce adipogenesis, another process known to be dependent on PPAR $\gamma$ . Indeed, pemafibrate induced adipogenesis in hMADS cells when added at the same concentration as rosiglitazone between D2 and D9. At the morphological level, pemafibrate-induced adipocytes appeared similar to those induced by rosiglitazone, albeit showing a lower triglyceride accumulation, and RNA and DNA content (Supplementary Fig. 3A, B and C). The mRNA levels of adipogenic markers FASN, GLUT1, and PLIN1 were similar in adipocyte induced by pemafibrate or rosiglitazone. However, the expression of FABP4 and lipases such as HSL or LPL was reduced in pemafibrate-induced adipocytes compared to those induced by rosiglitazone (Supplementary Fig. 3D). Our observations are reinforced by experiments intended to



indicate that pemafibrate, although known as a potent PPAR $\alpha$  agonist, induces adipocyte beiging and differentiation through the activation of PPAR $\gamma$ .

## 4. Discussion

This study investigates the role of PPAR $\alpha$  and its activation in human model for both adipogenesis and adipocyte being. While previous studies have put in evidence that hepatic PPAR $\alpha$  activation was crucial for WAT being, direct effect of PPAR $\alpha$  activation in adipocyte remains unclear, especially in human. Fibrates have been developed and used since the 1960s as hypolipidemic agents via hepatic PPAR $\alpha$  activation



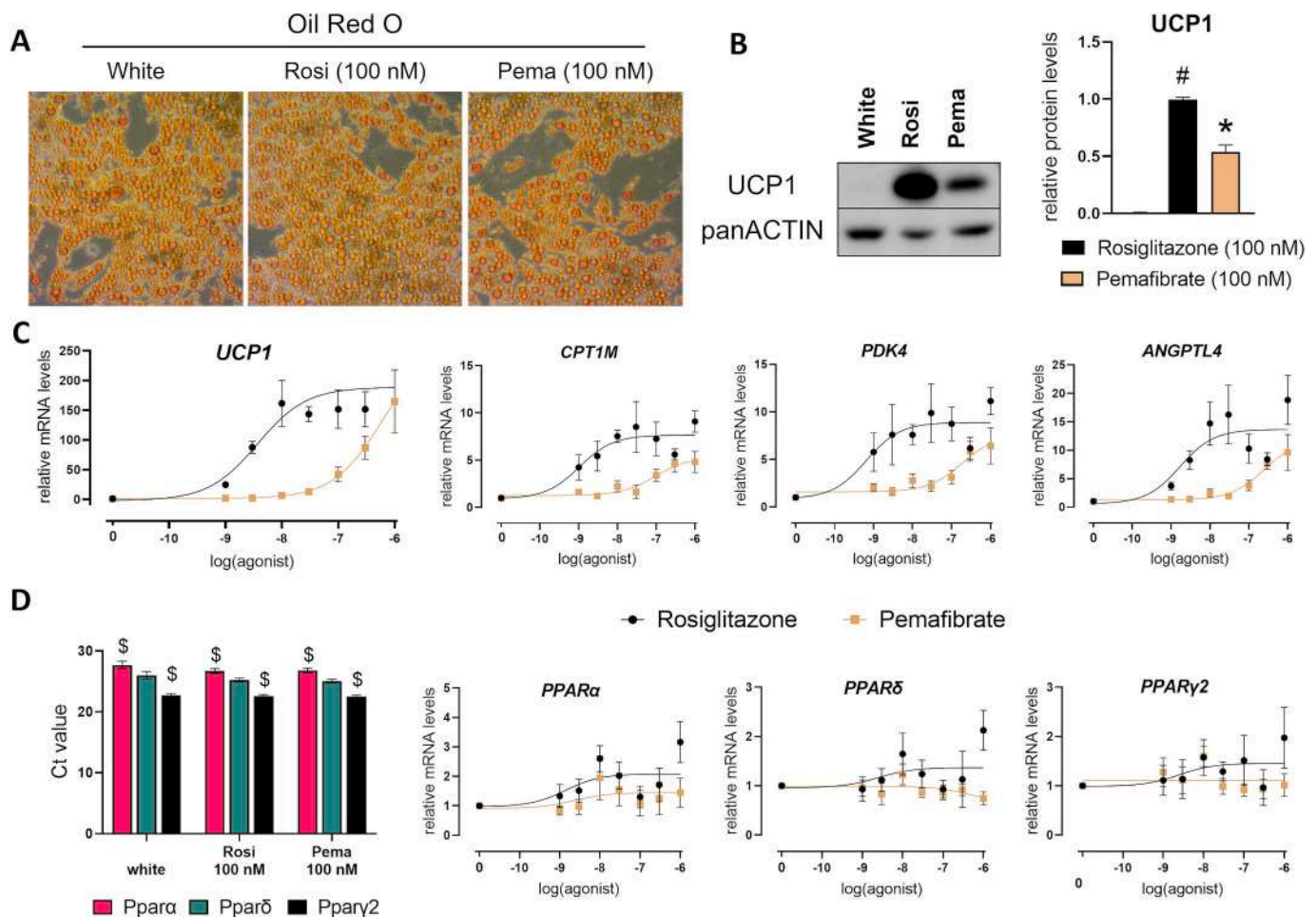


**Fig. 5.** Pemaifibrate induces UCP1 expression in human white adipocytes.

hMADS cells were induced to differentiate into adipocyte. At D14, hMADS adipocytes, considered as white adipocytes were converted for four days into thermogenic adipocytes using rosiglitazone or pemaifibrate, specific agonists of PPAR $\gamma$  and PPAR $\alpha$ , respectively. (A) Oil red O staining. (B) UCP1 protein expression. (C) *UCP1*, *CPT1M*, *PDK4* and *ANGPTL4* mRNA levels were measured upon treatment with various amounts of rosiglitazone or pemaifibrate. (D) PPARs mRNA levels either as Ct values or relative expression. Histograms display mean  $\pm$  SEM of 4 (B), 4–8 (C, D) independent experiments. Statistics by one-way ANOVA with Sidak multiple comparisons test,  $p < 0.05$  considered as significant: #, vs white siCtrl; \*, Pemaifibrate vs Rosiglitazone, \$, vs Ppar $\delta$ .

[41–44]. Fenofibrate is unable to induce the conversion of hMADS adipocytes toward a thermogenic phenotype (data not shown). In humans, pemaifibrate has been recently approved in Japan for the treatment of hyperlipidemia. However, no study investigated the role of pemaifibrate in human adipocytes.

Our results demonstrate that pemaifibrate is able to induce *UCP1* expression in two different models of human adipocytes. This in vitro approach avoids the pleiotropic effects of pemaifibrate on other cell types, as reported previously. Indeed, several studies have put in evidence that pemaifibrate might act on adipocyte thermogenic capacity by increasing liver and plasma FGF21 levels in mice [27,28]. Beneficial effect of pemaifibrate on the WAT thermogenic program are absent in FGF21 KO mice [27]. FGF21 induction mediated by PPAR $\alpha$  activation in liver is crucial to improve whole-body glucose metabolism in obese mice [45]. Here we show that pemaifibrate induces *UCP1* expression in human adipocytes. hMADS adipocytes do express *FGFR1* and *KLB* but display very low levels of *FGF21*. In our hands, FGF21 treatment failed to increase UCP1 expression in hMADS adipocytes (data not shown).

We show that pemaifibrate, an agonist supposedly specific for PPAR $\alpha$ , induces UCP1 expression even in the absence of PPAR $\alpha$ . Moreover, this induction is inhibited by PPAR $\gamma$  antagonist GW9662. These results highly suggest that pemaifibrate-dependent *UCP1* expression in adipocyte is more likely due to PPAR $\gamma$  activation, rather than PPAR $\alpha$  activation. This study also demonstrates that pemaifibrate is able to induce

adipogenesis, another process under the control of PPAR $\gamma$ . We confirm that pemaifibrate-dependent adipogenesis is mediated by PPAR $\gamma$  activation as it is not affected by the inhibition of PPAR $\alpha$  but completely suppressed by PPAR $\gamma$  silencing. In vivo, pemaifibrate could drive the secretion of hepatic FGF21 by activating PPAR $\alpha$  while simultaneously activating PPAR $\gamma$  in adipose tissue. In the latter, pemaifibrate seems to be a potent activator of PPAR $\gamma$ . Although several crystal structures of PPAR $\alpha$ -Ligand Binding Domain (LBD) [17,40,46] with pemaifibrate are available in the Protein Data Bank, more studies in physiological context are needed to better understand the effects of pemaifibrate. Altogether, our data questions the specificity of pemaifibrate and indicates that pemaifibrate represents a PPAR $\gamma$  activator in an adipocyte context.

PPAR $\gamma$  synthetic agonists such as rosiglitazone can induce the thermogenic program in mice WAT and the white-to-beige conversion in human adipocytes [8,31]. Thiazolidinediones used as insulin sensitizer, such as pioglitazone and rosiglitazone, have been associated with body weight gain attributed to increased fat mass, especially for subcutaneous depots, and associated with adverse effects such as heart failure [47]. These molecules are no longer appropriate for clinical use. Moreover, several studies have shown that dual PPAR $\alpha/\gamma$  activation is superior to selective PPAR $\gamma$  activation at inducing white fat browning in vivo [48,49]. Mechanistically, the superiority of dual PPAR $\alpha/\gamma$  activators is mediated at least in part via a PPAR $\alpha$ -driven increase in FGF21. Combined treatment with rosiglitazone and FGF21 results in a synergistic



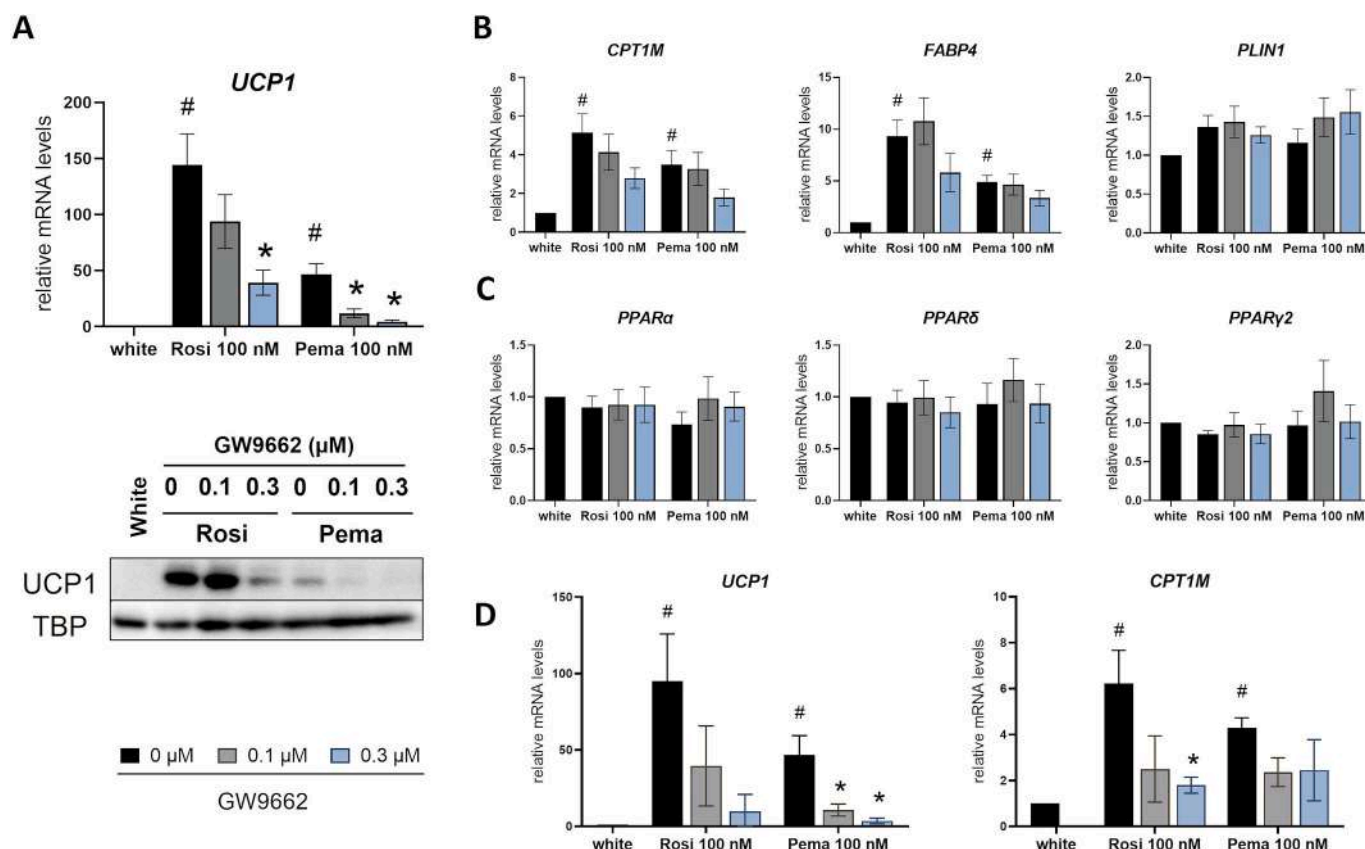


**Fig. 6.** PPAR $\gamma$  antagonist GW9662 interferes with PPAR $\alpha$  activation by pemafibrate. hMADS cells were induced to differentiate into adipocyte, and at D14 cells were induced or not to convert into thermogenic adipocytes using 100 nM rosiglitazone or 100 nM pemafibrate in the absence or the presence of GW9662, a PPAR $\gamma$  antagonist. (A) UCP1 mRNA and protein levels were measured. (B) CPT1M, FABP4, PLIN1 and (C) PPARs, mRNA levels were measured. (D) UCP1 and CPT1M mRNA expression in hSVF cells differentiated into adipocytes and treated with either rosiglitazone or pemafibrate in the absence or the presence of GW9662. Histograms display mean  $\pm$  SEM of 7 independent (A, B, C) or 3 (D) experiments.

Statistics by one-way ANOVA with Sidak multiple comparisons test,  $p < 0.05$  considered as significant: #, vs white; \*, vs untreated.

increase in UCP1 mRNA levels both in vitro and in vivo. However, several dual PPAR $\alpha/\gamma$  agonists have been shown to induce tumors in rodents. Tesaglitazar is a dual PPAR $\alpha/\gamma$  agonist that is more potent on PPAR $\gamma$  than on PPAR $\alpha$ . Tesaglitazar and muraglitazar, showing improved metabolic parameters, were abandoned when clinical trials showed either increased risk for cardiovascular events or other adverse effects, such as increased peripheral edema and creatine phosphokinase. Tesaglitazar causes cardiac dysfunction by inhibiting SIRT1-PGC1 $\alpha$  axis [50]. Pemafibrate could be a new dual PPAR $\alpha/\gamma$  activation but with a good safety profile.

Using human cell models, we also show herein that rosiglitazone treatment leads to an enhanced expression of UCP1 in the absence of PPAR $\alpha$ . However, our RNAseq data did not allow the identification of the involved mechanisms. Thus, it is tempting to speculate that PPAR $\alpha$  might interfere at a transcriptional level in the protein complexes to compete with PPAR $\gamma$  in the recruitment of coregulators at the distal enhancer part of the promoter [51]. Further studies are necessary to shed light on the involved mechanisms. PPAR $\gamma$  is an important regulator of both white and brown adipocyte differentiation and function. By contrast, PPAR $\alpha$  seems to be dispensable for adipogenesis and beiging. PPAR $\alpha$  may probably play a negative role for UCP1 expression mediated by PPAR $\gamma$  activation. Pemafibrate can induce adipogenesis and UCP1 expression in adipocyte more likely due to PPAR $\gamma$  activation, rather than PPAR $\alpha$  activation. However, these effects are weaker compared to rosiglitazone treatment. To date, no adverse effect associated to with PPAR $\gamma$  activation has been reported with pemafibrate use, and pemafibrate treatment ameliorated lipids abnormalities in patients with type 2 diabetes [51]. Our data identify pemafibrate as a potential therapeutic

tool to control body weight and metabolic disorders, most probably without the secondary effects of rosiglitazone and withdrawn dual PPAR $\alpha/\gamma$  activators.

## 5. Conclusion

This study investigates the role of PPAR $\alpha$  and its activation in beiging of human adipocytes. We show that PPAR $\alpha$  expression in adipocytes is a hindrance for PPAR $\gamma$ -induced UCP1 expression and that pemafibrate is a PPAR $\gamma$  agonist for adipogenesis and beiging. These observations are in favor of a crucial role of pemafibrate in the white-to-beige adipocyte conversion.

Supplementary data to this article can be found online at <https://doi.org/10.1016/j.lfs.2025.123406>.

## CRedit authorship contribution statement

**Pierre-Louis Batrow:** Writing – review & editing, Writing – original draft, Visualization, Validation, Methodology, Investigation, Formal analysis. **Christian H. Roux:** Visualization, Validation, Methodology, Formal analysis. **Nadine Gautier:** Writing – review & editing, Validation, Methodology, Data curation. **Luc Martin:** Validation, Investigation, Formal analysis. **Brigitte Sibille:** Visualization, Validation, Methodology, Formal analysis. **Hervé Guillou:** Visualization, Validation, Methodology, Formal analysis. **Catherine Postic:** Visualization, Validation, Methodology, Formal analysis. **Dominique Langin:** Visualization, Validation, Methodology, Formal analysis. **Isabelle Mothe-Satney:** Writing – review & editing, Writing – original draft,

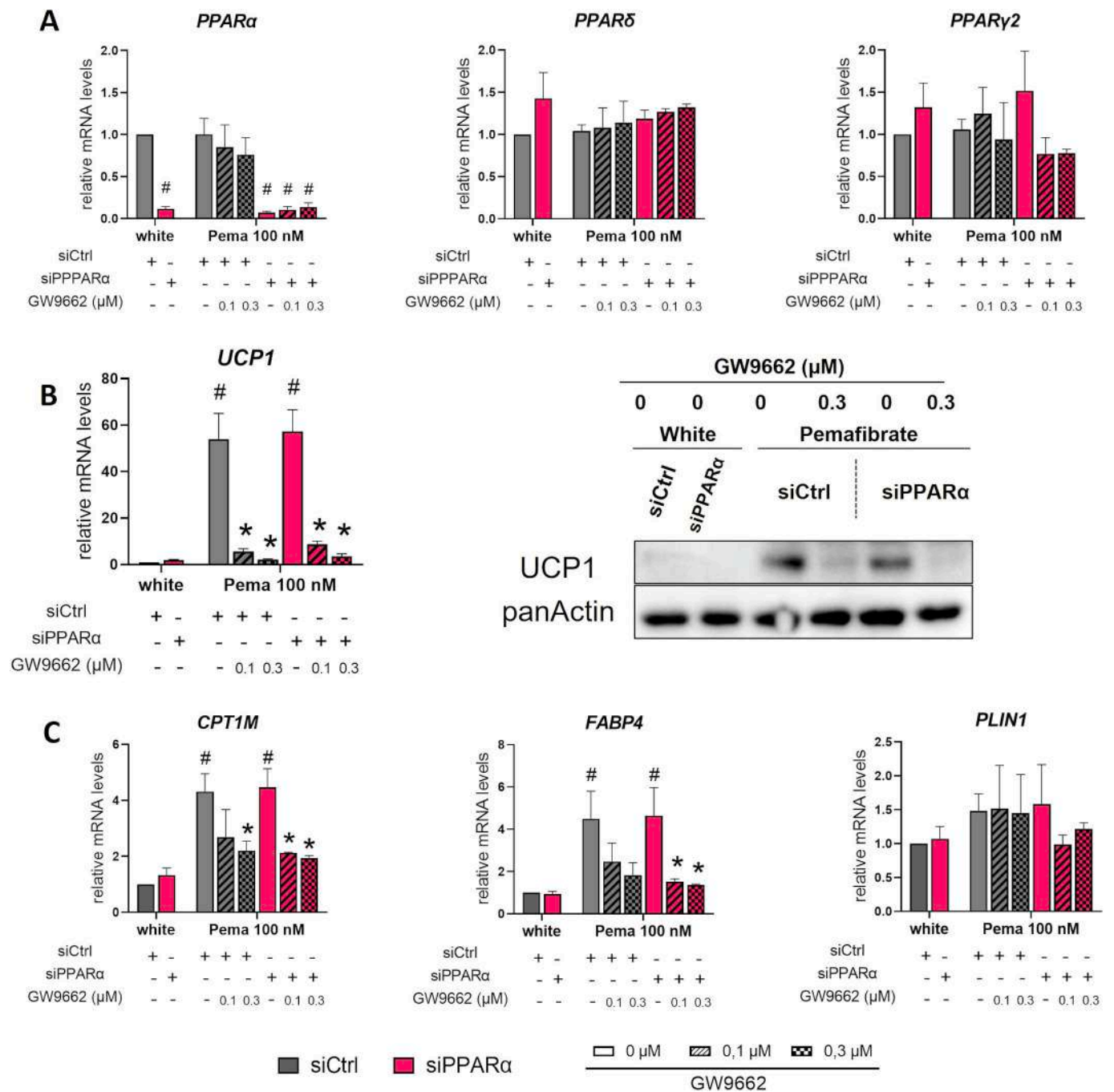


**Fig. 7.** Pemafibrate-dependent UCP1 induction is likely due to PPAR $\gamma$  activation. hMADS cells were induced to differentiate into adipocyte, were transfected with siRNA (siCtrl or siPPAR $\alpha$ ) at D10 and at D14 cells were treated or not for 4 days with 100 nM pemafibrate in the absence or the presence of GW9662, a PPAR $\gamma$  antagonist. (A) PPARs mRNA levels were measured, (B) UCP1 mRNA and protein, (C) CPT1M, FABP4 and PLIN1 mRNA levels were measured. Histograms display mean  $\pm$  SEM of 3 independent experiments. Statistics by one-way ANOVA with Sidak multiple comparisons test,  $p < 0.05$  considered as significant: #, vs white siCtrl; \*, vs untreated.

Visualization, Validation, Methodology, Investigation, Formal analysis. Ez-Zoubir Amri: Writing – review & editing, Writing – original draft, Funding acquisition, Data curation, Conceptualization.

**Declaration of competing interest**

The authors declare that they have no known competing financial interests or personal relationships that could have appeared to influence the work reported in this paper.

**Acknowledgments**

This work was supported by CNRS, Inserm and by “HepAdialogue” from the French National Research Agency (ANR) ANR-17-CE14-0015, “AdipoPiezo” (ANR-19-CE14-0029) and by the Nutricia Research Foundation. PLB is supported by grants from ANR and Université Côte d’Azur (ATER). This work was realized through the Adipo-Cible Research Study Group, supported by the French government through the France 2030 investment plan managed by the National Research Agency (ANR), as part of the Initiative of Excellence of Université Côte

d'Azur under reference number ANR-15-IDEX-01. We thank Dr. Vanessa Lanoue for editing the manuscript.

## Data availability

Data will be made available on request.

## References

- [1] N.C.D.R.F. Collaboration, Worldwide trends in underweight and obesity from, To 2022: a pooled analysis of 3663 population-representative studies with 222 million children, adolescents, and adults, *Lancet* 403 (2024) 1027–1050, [https://doi.org/10.1016/S0140-6736\(23\)02750-2](https://doi.org/10.1016/S0140-6736(23)02750-2).
- [2] S. Cinti, Adipose tissues and obesity, *Ital. J. Anat. Embryol.* 104 (1999) 37–51.
- [3] S. Cinti, Anatomy of the adipose organ, *Eat. Weight Disord.* 5 (2000) 132–142.
- [4] B. Cannon, J. Nedergaard, Brown adipose tissue: function and physiological significance, *Physiol. Rev.* 84 (2004) 277–359, <https://doi.org/10.1152/physrev.00015.2003> 84/1/277.
- [5] J.F. Rahbani, J. Bunk, D. Lagarde, B. Samborska, A. Roesler, H. Xiao, A. Shaw, Z. Kaiser, J.L. Braun, M.S. Geromella, V.A. Fajardo, R.A. Koza, L. Kazak, Parallel control of cold-triggered adipocyte thermogenesis by UCP1 and CKB, *Cell Metab.* 36 (2024) 526–540 e527, <https://doi.org/10.1016/j.cmet.2024.01.001>.
- [6] A. Vargas-Castillo, Y. Sun, A.L. Smythers, L. Grauvogel, P.A. Dumesic, M.P. Emont, L.T. Tsai, E.D. Rosen, N.W. Zammitt, S.M. Shaffer, M. Ordonez, E.T. Chouchani, S. P. Gygi, T. Wang, A.K. Sharma, M. Balaz, C. Wolfrum, B.M. Spiegelman, Development of a functional beige fat cell line uncovers independent subclasses of cells expressing UCP1 and the futile creatine cycle, *Cell Metab.* 36 (2024) 2146–2155 e2145, <https://doi.org/10.1016/j.cmet.2024.07.002>.
- [7] T. Wang, A.K. Sharma, C. Wu, C.I. Maushart, A. Ghosh, W. Yang, P. Stefanicka, Z. Kovanicova, J. Ukropec, J. Zhang, M. Arnold, M. Klug, K. De Bock, U. Schneider, C. Popescu, B. Zheng, L. Ding, F. Long, R.S. Dewal, C. Moser, W. Sun, H. Dong, M. Takes, D. Suelberg, A. Mameghani, A. Nocito, C.J. Zech, A. Chirindel, D. Wild, I. A. Burger, M.R. Schon, A. Dietrich, M. Gao, M. Heine, Y. Sun, A. Vargas-Castillo, S. Soberg, C. Scheele, M. Balaz, M. Blüher, M.J. Betz, B.M. Spiegelman, C. Wolfrum, Single-nucleus transcriptomics identifies separate classes of UCP1 and futile cycle adipocytes, *Cell Metab.* 36 (2024) 2130–2145 e2137, <https://doi.org/10.1016/j.cmet.2024.07.005>.
- [8] N. Petrovic, T.B. Walden, I.G. Shabalina, J.A. Timmons, B. Cannon, J. Nedergaard, Chronic peroxisome proliferator-activated receptor gamma (PPARGamma) activation of epididymally derived white adipocyte cultures reveals a population of thermogenically competent, UCP1-containing adipocytes molecularly distinct from classic brown adipocytes, *J. Biol. Chem.* 285 (2010) 7153–7164, <https://doi.org/10.1074/jbc.M109.053942>.
- [9] J. Nedergaard, T. Bengtsson, B. Cannon, Unexpected evidence for active brown adipose tissue in adult humans, *Am. J. Physiol. Endocrinol. Metab.* 293 (2007) E444–E452.
- [10] K.A. Virtanen, M.E. Lidell, J. Orava, M. Heglind, R. Westergren, T. Niemi, M. Taittonen, J. Laine, N.J. Savisto, S. Enerback, P. Nuutila, Functional brown adipose tissue in healthy adults, *N. Engl. J. Med.* 360 (2009) 1518–1525.
- [11] A.M. Cypess, S. Lehman, G. Williams, I. Tal, D. Rodman, A.B. Goldfine, F.C. Kuo, E. L. Palmer, Y.H. Tseng, A. Doria, G.M. Kolodny, C.R. Kahn, Identification and importance of brown adipose tissue in adult humans, *N. Engl. J. Med.* 360 (2009) 1509–1517.
- [12] M. Rosenwald, A. Perdikari, T. Rulicke, C. Wolfrum, Bi-directional interconversion of brite and white adipocytes, *Nat. Cell Biol.* 15 (2013) 659–667, <https://doi.org/10.1038/ncb2740>.
- [13] Q.A. Wang, C. Tao, R.K. Gupta, P.E. Scherer, Tracking adipogenesis during white adipose tissue development, expansion and regeneration, *Nat. Med.* 19 (2013) 1338–1344, <https://doi.org/10.1038/nm.3324>.
- [14] P. Corrales, A. Vidal-Puig, G. Medina-Gomez, PPARs and metabolic disorders associated with challenged adipose tissue plasticity, *Int. J. Mol. Sci.* 19 (2018), <https://doi.org/10.3390/ijms19072124>.
- [15] S. Kersten, Peroxisome proliferator activated receptors and obesity, *Eur. J. Pharmacol.* 440 (2002) 223–234, [https://doi.org/10.1016/S0014-2999\(02\)01431-0](https://doi.org/10.1016/S0014-2999(02)01431-0).
- [16] K. Schoonjans, B. Staels, J. Auwerx, Role of the peroxisome proliferator-activated receptor (PPAR) in mediating the effects of fibrates and fatty acids on gene expression, *J. Lipid Res.* 37 (1996) 907–925.
- [17] S. Kamata, T. Oyama, K. Saito, A. Honda, Y. Yamamoto, K. Suda, R. Ishikawa, T. Itoh, Y. Watanabe, T. Shibata, K. Uchida, M. Suematsu, I. Ishii, PPARalpha ligand-binding domain structures with endogenous fatty acids and fibrates, *iScience*. 23 (2020) 101727, <https://doi.org/10.1016/j.isci.2020.101727>.
- [18] V. Barquissau, D. Beuzelin, D.F. Pisani, G.E. Beranger, A. Mairal, A. Montagner, B. Roussel, G. Tavernier, M.A. Marques, C. Moro, H. Guillou, E.Z. Amri, D. Langin, White-to-brite conversion in human adipocytes promotes metabolic reprogramming towards fatty acid anabolic and catabolic pathways, *Mol. Metab.* 5 (2016) 352–365, <https://doi.org/10.1016/j.molmet.2016.03.002>.
- [19] B. Xu, A. Xing, S. Li, The forgotten type 2 diabetes mellitus medicine: rosiglitazone, *Diabetol. Int.* 13 (2022) 49–65, <https://doi.org/10.1007/s13340-021-00519-0>.
- [20] R.V. Giglio, N. Papanas, A.A. Rizvi, M. Ciccio, A.M. Patti, I. Ilias, A. Pantea Stoian, A. Sahebkar, A. Jazey, M. Rizzo, An update on the current and emerging use of Thiazolidinediones for type 2 diabetes, *Medicina (Kaunas)* 58 (2022), <https://doi.org/10.3390/medicina58101475>.
- [21] B. De Filippis, A. Granese, A. Ammazalorso, Peroxisome proliferator-activated receptor agonists and antagonists: an updated patent review (2020–2023), *Expert Opin. Ther. Pat.* (2024) 1–16, <https://doi.org/10.1080/13543776.2024.2332661>.
- [22] Z. Changizi, F. Kajbaf, A. Moslehi, An overview of the role of peroxisome proliferator-activated receptors in liver diseases, *J. Clin. Transl. Hepatol.* 11 (2023) 1542–1552, <https://doi.org/10.14218/JCTH.2023.00334>.
- [23] N. Hennuyer, I. Duplan, C. Paquet, J. Vanhoutte, E. Woittrain, V. Touche, S. Colin, E. Vallez, S. Lestavel, P. Lefebvre, B. Staels, The novel selective PPARalpha modulator (SPPARMalpha) pemafibrate improves dyslipidemia, enhances reverse cholesterol transport and decreases inflammation and atherosclerosis, *Atherosclerosis* 249 (2016) 200–208, <https://doi.org/10.1016/j.atherosclerosis.2016.03.003>.
- [24] Y. Honda, T. Kessoku, Y. Ogawa, W. Tomeno, K. Imajo, K. Fujita, M. Yoneda, T. Takizawa, S. Saito, Y. Nagashima, A. Nakajima, Pemafibrate, a novel selective peroxisome proliferator-activated receptor alpha modulator, improves the pathogenesis in a rodent model of nonalcoholic steatohepatitis, *Sci. Rep.* 7 (2017) 42477, <https://doi.org/10.1038/srep42477>.
- [25] S. Ishibashi, S. Yamashita, H. Arai, E. Araki, K. Yokote, H. Suganami, J.C. Fruchart, T. Kodama, K.S. Group, Effects of K-877, a novel selective PPARalpha modulator (SPPARMalpha), in dyslipidaemic patients: a randomized, double blind, active- and placebo-controlled, phase 2 trial, *Atherosclerosis* 249 (2016) 36–43, <https://doi.org/10.1016/j.atherosclerosis.2016.02.029>.
- [26] H.A. Blair, Pemafibrate: first global approval, *Drugs* 77 (2017) 1805–1810, <https://doi.org/10.1007/s40265-017-0818-x>.
- [27] M. Araki, Y. Nakagawa, A. Oishi, S.I. Han, Y. Wang, K. Kumagai, H. Ohno, Y. Mizunoe, H. Iwasaki, M. Sekiya, T. Matsuzaka, H. Shimano, The peroxisome proliferator-activated receptor alpha (PPARalpha) agonist Pemafibrate protects against diet-induced obesity in mice, *Int. J. Mol. Sci.* 19 (2018), <https://doi.org/10.3390/ijms19072148>.
- [28] G. Egusa, H. Ohno, G. Nagano, J. Sagawa, H. Shinjo, Y. Yamamoto, N. Himeno, Y. Morita, A. Kanai, R. Baba, K. Kobuke, K. Oki, M. Yoneda, N. Hattori, Selective activation of PPARalpha maintains thermogenic capacity of beige adipocytes, *iScience*. 26 (2023) 107143, <https://doi.org/10.1016/j.isci.2023.107143>.
- [29] A.M. Rodriguez, C. Elabd, E.Z. Amri, G. Ailhaud, C. Dani, The human adipose tissue is a source of multipotent stem cells, *Biochimie* 87 (2005) 125–128, <https://doi.org/10.1016/j.biochi.2004.11.007>.
- [30] A.M. Rodriguez, D. Pisani, C.A. Dechesne, C. Turc-Carel, J.Y. Kurzenne, B. Wdziekowski, A. Villageois, C. Bagnis, J.P. Breitmayer, H. Groux, G. Ailhaud, C. Dani, Transplantation of a multipotent cell population from human adipose tissue induces dystrophin expression in the immunocompetent mdx mouse, *J. Exp. Med.* 201 (2005) 1397–1405, <https://doi.org/10.1084/jem.20042224>.
- [31] C. Elabd, C. Chiellini, M. Carmona, J. Galitzky, O. Cochet, R. Petersen, L. Penicaud, K. Kristiansen, A. Bouloumie, L. Castella, C. Dani, G. Ailhaud, E.Z. Amri, Human multipotent adipose-derived stem cells differentiate into functional brown adipocytes, *Stem Cells* 27 (2009) 2753–2760.
- [32] R.A. Ghandour, M. Giroud, A. Vegiopoulos, S. Herzig, G. Ailhaud, E.Z. Amri, D. F. Pisani, IP-receptor and PPARs trigger the conversion of human white to brite adipocyte induced by carbaprostacyclin, *Biochim. Biophys. Acta* 2016 (1861) 285–293, <https://doi.org/10.1016/j.bbap.2016.01.007>.
- [33] D.F. Pisani, V. Barquissau, J.C. Chambard, D. Beuzelin, R.A. Ghandour, M. Giroud, A. Mairal, S. Pagnotta, S. Cinti, D. Langin, E.Z. Amri, Mitochondrial fission is associated with UCP1 activity in human brite/beige adipocytes, *Molecular metabolism*. 7 (2018) 35–44, <https://doi.org/10.1016/j.molmet.2017.11.007>.
- [34] D.F. Pisani, G.E. Beranger, A. Corinus, M. Giroud, R.A. Ghandour, J. Altirriba, J. C. Chambard, N.M. Mazure, S. Bendahhou, C. Duranton, J.F. Michiels, A. Frontini, F. Rohner-Jeanrenaud, S. Cinti, M. Christian, J. Barhanin, E.Z. Amri, The K+ channel TASK1 modulates beta-adrenergic response in brown adipose tissue through the mineralocorticoid receptor pathway, *FASEB J.* 30 (2016) 909–922, <https://doi.org/10.1096/fj.15-277475>.
- [35] M. Rodbell, Metabolism of isolated fat cells. I. Effects of hormones on glucose metabolism and lipolysis, *J. Biol. Chem.* 239 (1964) 375–380.
- [36] D.F. Pisani, M. Djedaini, G.E. Beranger, C. Elabd, M. Scheideler, G. Ailhaud, E. Z. Amri, Differentiation of human adipose-derived stem cells into “Brite” (Brown-in-white) adipocytes, *Front. Endocrinol. (Lausanne)*. 2 (2011) 87, <https://doi.org/10.3389/fendo.2011.00087>.
- [37] S.X. Ge, E.W. Son, R. Yao, iDEP: an integrated web application for differential expression and pathway analysis of RNA-Seq data, *BMC Bioinformatics*. 19 (2018) 534, <https://doi.org/10.1186/s12859-018-2486-6>.
- [38] D.F. Pisani, R.A. Ghandour, G.E. Beranger, P. Le Faouder, J.C. Chambard, M. Giroud, A. Vegiopoulos, M. Djedaini, J. Bertrand-Michel, M. Tauc, S. Herzig, D. Langin, G. Ailhaud, C. Duranton, E.Z. Amri, The omega-6-fatty acid, arachidonic acid, regulates the conversion of white to brite adipocyte through a prostaglandin/calcium mediated pathway, *Mol. Metab.* 3 (2014) 834–847, <https://doi.org/10.1016/j.molmet.2014.09.003>.
- [39] N. Ferri, A. Corsini, C. Sirtori, M. Ruscica, PPAR-alpha agonists are still on the rise: an update on clinical and experimental findings, *Expert Opin. Investig. Drugs* 26 (2017) 593–602, <https://doi.org/10.1080/13543784.2017.1312339>.
- [40] Y. Yamamoto, K. Takei, S. Arulmozhiraja, V. Sladek, N. Matsuo, S.I. Han, T. Matsuzaka, M. Sekiya, T. Tokiwa, M. Shoji, Y. Shigeta, Y. Nakagawa, H. Tokiwa, H. Shimano, Molecular association model of PPARalpha and its new specific and efficient ligand, pemafibrate: structural basis for SPPARMalpha, *Biochem. Biophys. Res. Commun.* 499 (2018) 239–245, <https://doi.org/10.1016/j.bbrc.2018.03.135>.
- [41] D. Montaigne, L. Butruille, B. Staels, PPAR control of metabolism and cardiovascular functions, *Nat. Rev. Cardiol.* 18 (2021) 809–823, <https://doi.org/10.1038/s41569-021-00569-6>.

- [42] S. Kersten, B. Desvergne, W. Wahli, Roles of PPARs in health and disease, *Nature* 405 (2000) 421–424, <https://doi.org/10.1038/35013000>.
- [43] S. Kersten, W. Wahli, Peroxisome proliferator activated receptor agonists, *EXS* 89 (2000) 141–151.
- [44] K.G. Green, W.H. Inman, J.M. Thorp, Multicentre trial in the United Kingdom and Ireland of a mixture of ethyl Chlorophenoxyisobutyrate and Androsterone (Atromid). A preliminary report, *J. Atheroscler. Res.* 3 (1963) 593–616, [https://doi.org/10.1016/s0368-1319\(63\)80043-5](https://doi.org/10.1016/s0368-1319(63)80043-5).
- [45] T. Goto, M. Hirata, Y. Aoki, M. Iwase, H. Takahashi, M. Kim, Y. Li, H.F. Jheng, W. Nomura, N. Takahashi, C.S. Kim, R. Yu, S. Seno, H. Matsuda, M. Aizawa-Abe, K. Ebihara, N. Itoh, T. Kawada, The hepatokine FGF21 is crucial for peroxisome proliferator-activated receptor- $\alpha$  agonist-induced amelioration of metabolic disorders in obese mice, *J. Biol. Chem.* 292 (2017) 9175–9190, <https://doi.org/10.1074/jbc.M116.767590>.
- [46] M. Kawasaki, A. Kambe, Y. Yamamoto, S. Arulmozhiraja, S. Ito, Y. Nakagawa, H. Tokiwa, S. Nakano, H. Shimano, Elucidation of molecular mechanism of a selective PPAR $\alpha$  modulator, Pemaifibrate, through combinational approaches of X-ray crystallography, thermodynamic analysis, and first-principle calculations, *Int. J. Mol. Sci.* 21 (2020), <https://doi.org/10.3390/ijms21010361>.
- [47] S.S. Choi, J. Park, J.H. Choi, Revisiting PPAR $\gamma$  as a target for the treatment of metabolic disorders, *BMB Rep.* 47 (2014) 599–608, <https://doi.org/10.5483/bmbrep.2014.47.11.174>.
- [48] T. Kroon, M. Harms, S. Maurer, L. Bonnet, I. Alexandersson, A. Lindblom, A. Ahnmark, D. Nilsson, P. Gennemark, G. O'Mahony, V. Osinski, C. McNamara, J. Boucher, PPAR $\gamma$  and PPAR $\alpha$  synergize to induce robust browning of white fat in vivo, *Mol. Metab.* 36 (2020) 100964, <https://doi.org/10.1016/j.molmet.2020.02.007>.
- [49] C.S. Miranda, F.M. Silva-Veiga, D.A. Santana-Oliveira, I.M.L. Vasques-Monteiro, J. B. Daleprane, V. Souza-Mello, PPAR $\alpha$ /gamma synergism activates UCP1-dependent and -independent thermogenesis and improves mitochondrial dynamics in the beige adipocytes of high-fat fed mice, *Nutrition* 117 (2024) 112253, <https://doi.org/10.1016/j.nut.2023.112253>.
- [50] C. Kalliora, I.D. Kyriazis, S.I. Oka, M.J. Lieu, Y. Yue, E. Area-Gomez, C.J. Pol, Y. Tian, W. Mizushima, A. Chin, D. Scerbo, P.C. Schulze, M. Civelek, J. Sadoshima, M. Madesh, I.J. Goldberg, K. Drosatos, Dual peroxisome-proliferator-activated-receptor- $\alpha$ /gamma activation inhibits SIRT1-PGC1 $\alpha$  axis and causes cardiac dysfunction, *JCI Insight* 5 (2019), <https://doi.org/10.1172/jci.insight.129556>.
- [51] E. Araki, S. Yamashita, H. Arai, K. Yokote, J. Satoh, T. Inoguchi, J. Nakamura, H. Maegawa, N. Yoshioka, Y. Tanizawa, H. Watada, H. Suganami, S. Ishibashi, Effects of Pemaifibrate, a novel selective PPAR $\alpha$  modulator, on lipid and glucose metabolism in patients with type 2 diabetes and hypertriglyceridemia: a randomized, double-blind, placebo-controlled, phase 3 trial, *Diabetes Care* 41 (2018) 538–546, <https://doi.org/10.2337/dc17-1589>.